Organic & Biomolecular Chemistry

Cite this: *Org. Biomol. Chem.*, 2011, **9**, 1201

www.rsc.org/obc

**PAPER**

# Reveromycins Revealed: New polyketide spiroketals from Australian marine-derived and terrestrial *Streptomyces* spp. A case of natural products *vs.* artifacts†

**Leith Fremlin,[a] Michelle Farrugia,[a] Andrew M. Piggott,[a] Zeinab Khalil,[a] Ernest Lacey[b] and Robert J. Capon*[a]**

***Received 1st September 2010, Accepted 29th October 2010***
**DOI: 10.1039/c0ob00654h**

Chemical analysis of fermentation products from two Australian *Streptomyces* isolates yielded all four known and twelve new examples of the rare reveromycin class of polyketide spiroketals, including hemi-succinates, hemi-fumarates and hemi-furanoates. Reveromycins were identified with the aid of HPLC-DAD-MS and HPLC-DAD-SPE-NMR methodology, and structures were assigned by detailed spectroscopic analysis. The structural and mechanistic requirements for an unprecedented hemi-succinate : ketal-succinyl equilibrium were defined and provided a basis for proposing that reveromycin 4′-methyl esters and 5,6-spiroketals were artifacts. A plausible reveromycin polyketide biosynthesis is proposed, requiring a 2-methylsuccinyl-CoA starter unit, with flexible incorporation of a $C_{6\text{-}8}$ polyketide chain extension and diacid esterification units. Structure activity relationship investigations by co-metabolites were used to assess the anticancer, antibacterial and antifungal properties of reveromycins.

## Introduction

The polyketide spiroketal reveromycins A–D (**1–4**) were first described from a Japanese soil *Streptomyces* sp. (SN-593) in the early 1990s by researchers from the RIKEN Antibiotics Laboratory.[1–4] At that time, and with only planar structures assigned, the 6,6-spiroketal reveromycins A, C and D (**1**, **3** and **4**) were shown to possess noteworthy biological activities, being cytotoxic to *Candida albicans* (3 μM MIC at pH 3.0, compared to 16 μM for fluconazole) and the human cancer KB and K562 cell lines ($IC_{50}$ ~3 μM, compared to 97 μM for 5-fluorouracil).[3] The 6,6-spiroketals **1**, **3** and **4** also inhibited epidermal growth factor induced mitogenic activity in Balb/MK cells ($IC_{50}$ ~1 μM), and induced morphological reversion of srcts-NRK cells ($EC_{50}$ ~2.4 μM).[3]

In an attempt to fully resolve the reveromycin structures, in 1994 Isono[5] reported on a chemical degradation and spectroscopic approach to the assignment of absolute configuration to **1**, while asymmetric total syntheses of **1** were reported in 2000 by Nakata[6] and 2004 by Rizzacasa.[7] The asymmetric total synthesis of the less biologically active 5,6-spiroketal **2** was described in the 1999 and 2000 reports by Theodorakis,[8,9] a 1999 report by Nakata[10] and in the 2000 and 2001 reports by Rizzacasa.[11,12] Despite multiple successful syntheses, reveromycin structure activity relationship (SAR) investigations have relied on modification of **1** sourced from microbial fermentation.[13,14] This latter observation is not surprising given the nature of the total syntheses and the fact that **1** is the major polyketide produced by *Streptomyces* sp. SN-593; a 100 L fermentation yielded **1** (3 g), **2** (12 mg), **3** (80 mg) and **4** (14 mg).[2] Notwithstanding the advantages of microbial fermentation, such SAR studies are limited by access to the producing organism and/or fermentation products, as well as the polyketide framework and functionality defined by **1**.

In this report, we describe investigations into the chemistry of two Australian actinomycetes, the marine-derived *Streptomyces* sp. MST-MA568 and the terrestrial *Streptomyces* sp. MST-RA7781, both of which produce known and new reveromycins. In addition to the four known reveromycins A–D (**1–4**), we report twelve new analogues spanning homologues of the 6,6-spiroketal [hemi-succinate E (**5**), the 4′-methyl esters of A, D and E (**8–10**), the hemi-fumarates H–J (**11–13**) and the hemi-furanoates K–M (**14–16**)] and 5,6-spiroketal [hemi-succinates F and G (**6** and **7**)] reveromycin motifs. What follows is an account of the isolation, characterization and structure elucidation of reveromycins **1–16**, extending to investigations into chemical stability, the formation of artifacts, as well as commentary on biosynthesis and biological activity.

[a]*Institute for Molecular Bioscience, The University of Queensland, St. Lucia, QLD, 4072, Australia. E-mail: r.capon@uq.edu.au; Fax: +61 7 3346 2090; Tel: + 61 7 3346 2979*

[b]*Microbial Screening Technologies, Building A, 28-54 Percival Rd, Smithfield, NSW, 2164, Australia. E-mail: elacey@microbialscreening.com; Fax: +61 2 9757 2586; Tel: +61 2 9757 4515*

† Electronic supplementary information (ESI) available: General experimental details, tabulated NMR data and $^1$H spectra for all compounds, bioassay results and microbial taxonomy. See DOI: 10.1039/c0ob00654h

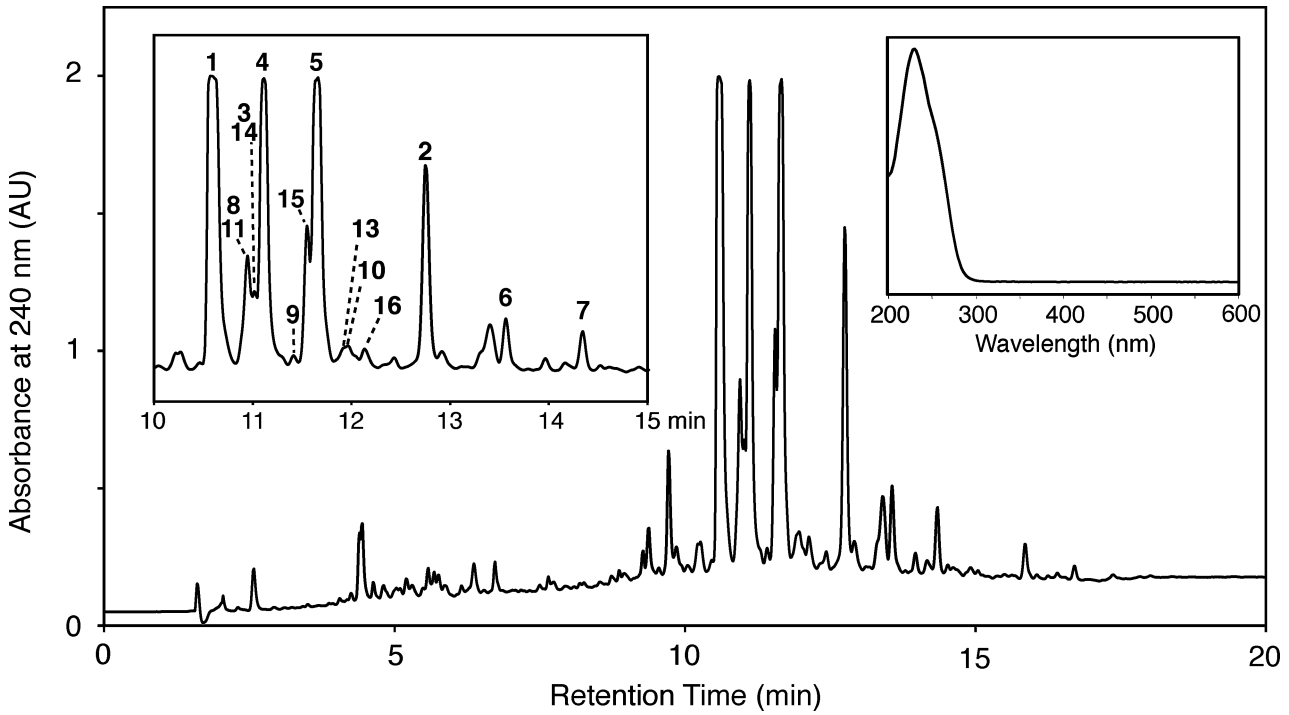


**Fig. 1** $C_{18}$ HPLC-DAD (240 nm) chromatogram of the crude extract from *Streptomyces* sp. MST-RA7781. Inset (top left) 10–15 min expansion. Inset (top right) UV-Vis spectrum of reveromycin A (**1**) (extracted from DAD data).

## Results and Discussion

### Chemical Profiling

During investigations into the chemistry of Australian microorganisms, we screened a large library of microbial extracts and detected rare and noteworthy chemical fingerprints (HPLC-DAD-MS) in extracts obtained from a marine-derived *Streptomyces* sp. (MST-MA568), isolated from a sediment sample collected near Nelson in the Glenelg River region of South Australia, and a rare terrestrial *Streptomyces* sp. (MST-RA7781), isolated from a soil sample collected near Temora, New South Wales. Careful analysis of the data suggested that both isolates produced reveromycins, a rare class of actinomycete spiroketal with natural occurrences limited to only four known analogues (**1–4**), all derived from a single Japanese *Streptomyces* sp. (SN-593). In our collection of 400 000 isolates, the incidence of actinomycetes producing reveromycins was low (1 in 20 000), while the incidence of isolates that produce at very high levels (such as MST-RA7781) was far lower (only 1 in the entire collection).

### Cultivation and Isolation

Solvent partitioning, followed by gel chromatography and $C_8$ HPLC fractionation on a scaled-up cultivation (1 L) of MST-MA568 returned low yields of the known reveromycin A (**1**), and a new homologue, reveromycin E (**5**) (Scheme S1, ESI†). By contrast, scaled-up cultivation (20 deep Petri plates) of MST-RA7781 returned far higher yields (>1000 fold compared to MST-MA568) of a highly complex mixture of reveromycins (Fig. 1). The complexity of this mixture challenged and defied traditional isolation techniques, prompting the consideration of alternative strategies. Fermentation products from MST-RA7781 were pre-fractionated by $C_{18}$ solid phase extraction (SPE) and preparative $C_{18}$ HPLC to yield five fractions. Two strategies were employed in an attempt to isolate and identify the full complement of reveromycins found within each of these fractions. In a traditional HPLC strategy, samples of each fraction were subjected to semi-preparative $C_8$ HPLC, to yield reveromycins A (**1**), C (**3**), D (**4**), E (**5**), E 4′-methyl ester (**10**) and J (**13**) (Scheme S2, ESI†). Significantly, this HPLC approach detected, but failed to resolve, a number of additional reveromycin co-metabolites.

To identify the remaining reveromycins, we adopted an HPLC-DAD-SPE-NMR approach, which involved: (i) 500 μg injections of each fraction through an analytical $C_8$ HPLC column, with DAD monitoring to select (*in situ*) eluting peaks of interest; (ii) robotic collection of peaks of interest onto individual microtitre plate SPE cartridges (PDVB), using post-column addition of $H_2O$ (*via* a secondary pump) to dilute the HPLC eluting solvent and prevent premature elution of the metabolites from the cartridges; (iii) robotic drying of the microtitre plate SPE cartridges with a stream of dry $N_2$; (iv) robotic elution of the metabolites from the SPE cartridges into the LC-NMR probe with a fixed aliquot of MeOH-$d_4$; (v) acquisition of 1D and 2D NMR spectra; (vi) elution of the metabolites from the probe with MeOH for recovery and further spectroscopic analysis (*i.e.* HRESI(±)MS).

Advantages of this HPLC-DAD-SPE-NMR strategy include: (a) the use of analytical HPLC to maximize resolution in the fractionation process; (b) the use of *in situ* robotics to coordinate handing of low mass samples, minimizing contamination risk; (c) the use of a high sensitivity, low volume LC-NMR probe to maximize sample concentration and NMR data quality. In our hands, this strategy was successfully employed to identify sixteen reveromycins, spanning the four known metabolites **1–4**, and twelve new analogues **5–16** (Scheme S3, ESI†). A detailed analysis

 

**Table 1** Comparative summary of $^{13}C$ NMR (MeOH-$d_4$) chemical shifts (ppm) for reveromycins

| | 6,6-spiro hemi-succinates | | | | 5,6-spiro hemi-succinates | | | 6,6-spiro 4′-methyl esters | | | 6,6-spiro hemi-fumarates | | 6,6-spiro hemi-furanoates | | |
|---|---|---|---|---|---|---|---|---|---|---|---|---|---|---|---|
| Pos. | A (**1**) | C (**3**) | D (**4**) | E (**5**) | B (**2**) | F (**6**) | G (**7**) | "A" (**8**) | "D" (**9**) | "E" (**10**) | H (**11**) | J (**13**) | K (**14**) | L (**15**) | M (**16**) |
| 1 | 169.8 | 169.9 | 169.9 | 170.2 | 169.7 | 169.8 | 169.7 | 169.5 | 170.3 | 170.2 | 170.3 | 169.3 | 169.9 | 170.1 | 170.1 |
| 2 | 122.3 | 122.3 | 122.4 | 122.5 | 120.9 | 120.9 | 120.9 | 122.3 | 122.7 | 122.3 | 122.7 | 122.5 | 122.7 | 122.4 | 122.1 |
| 3 | 152.7 | 152.6 | 152.9 | 152.8 | 152.8 | 152.8 | 152.8 | 152.8 | 152.5 | 152.9 | 153.8 | 152.5 | 153.0 | 152.6 | 152.4 |
| 4 | 43.9 | 43.9 | 44.2 | 44.1 | 43.8 | 44.0 | 43.9 | 43.9 | 44.3 | 44.0 | 44.3 | 44.0 | 44.3 | 44.0 | 43.9 |
| 5 | 76.7 | 76.7 | 76.8 | 76.9 | 76.9 | 76.9 | 76.9 | 76.7 | 77.1 | 76.8 | 77.1 | 76.7 | 77.1 | 76.8 | 76.6 |
| 6 | 127.7 | 127.7 | 128.0 | 127.8 | 126.9 | 127.0 | 127.1 | 127.8 | 128.1 | 127.8 | 128.1 | 127.8 | 128.1 | 127.9 | 127.6 |
| 7 | 137.7 | 137.7 | 137.9 | 137.8 | 138.4 | 138.4 | 138.4 | 137.7 | 137.9 | 137.7 | 138.0 | 137.6 | 138.0 | 137.5 | 137.4 |
| 8 | 135.9 | 135.3 | 135.3 | 135.2 | 135.2 | 135.8 | 135.1 | 135.1 | 135.6 | 135.6 | 135.4 | 135.0 | 134.2 | 135.4 | 135.7 |
| 9 | 129.3 | 129.2 | 129.5 | 129.4 | 130.7 | 130.7 | 130.7 | 129.4 | 129.6 | 129.3 | 129.5 | 129.1 | 129.5 | 129.1 | 129.0 |
| 10 | 32.8 | 32.8 | 32.9 | 32.9 | 32.7 | 32.8 | 32.5 | 32.7 | 32.9 | 32.8 | 34.9 | 32.8 | 33.1 | 32.7 | 32.7 |
| 11 | 76.1 | 76.1 | 76.2 | 76.2 | 78.3 | 78.3 | 78.4 | 76.2 | 76.4 | 76.2 | 76.5 | 76.2 | 76.5 | 76.1 | 75.9 |
| 12 | 36.2 | 36.2 | 34.8 | 34.6 | 35.6 | 35.6 | 35.5 | 34.6 | 34.9 | 34.8 | 34.9 | 34.6 | 34.5 | 34.7 | 34.5 |
| 13 | 28.1 | 28.1 | 28.7 | 28.6 | 30.1 | 30.2 | 30.2 | 28.5 | 28.8 | 28.3 | 29.7 | 28.5 | 28.9 | 28.4 | 28.4 |
| 14 | 36.7 | 36.8 | 36.8 | 36.8 | 35.1 | 35.2 | 35.2 | 36.8 | 37.1 | 36.7 | 37.3 | 36.9 | 37.3 | 37.1 | 37.0 |
| 15 | 97.1 | 96.9 | 96.9 | 97.1 | 108.7 | 108.8 | 108.9 | 96.7 | 97.1 | 96.3 | 97.1 | # | 97.1 | # | # |
| 16 | 35.1 | 35.1 | 32.8 | 32.6 | 39.5 | 39.6 | 39.5 | 35.1 | 33.2 | 32.5 | 33.0 | 32.7 | 32.7 | 32.9 | 32.6 |
| 17 | 25.4 | 25.2 | 25.3 | 25.3 | 32.8 | 32.7 | 32.8 | 25.1 | 25.6 | 25.3 | 25.6 | 25.2 | 25.4 | 25.3 | 25.3 |
| 18 | 84.2 | 84.0 | 83.9 | 84.1 | 88.5 | 88.6 | 88.7 | 84.2 | 84.5 | 84.0 | 85.4 | # | 85.2 | # | # |
| 19 | 79.5 | 79.7 | 79.7 | 79.8 | 80.2 | 80.3 | 80.2 | 79.5 | 79.9 | 79.7 | 79.9 | 79.6 | 80.1 | 79.8 | 79.8 |
| 20 | 134.1 | 133.8 | 134.2 | 134.1 | 132.4 | 132.4 | 132.4 | 133.9 | 134.2 | 134.2 | 134.1 | 133.5 | 134.1 | 133.8 | 133.6 |
| 21 | 139.1 | 139.1 | 139.1 | 139.1 | 135.4 | 135.8 | 135.7 | 139.2 | 139.4 | 139.2 | 139.8 | 139.5 | 139.8 | 139.4 | 139.4 |
| 22 | 152.6 | 152.6 | 152.5 | 152.3 | 152.3 | 152.2 | 152.7 | 151.6 | 152.9 | 152.5 | 153.0 | 151.9 | 152.3 | 152.1 | 152.4 |
| 23 | 121.3 | 121.4 | 121.6 | 121.5 | 122.2 | 122.2 | 122.3 | 121.4 | 121.9 | 121.6 | 122.0 | 121.5 | 121.9 | 121.4 | 121.5 |
| 24 | 170.0 | 170.0 | 169.7 | 169.9 | 169.7 | 170.1 | 170.3 | 169.5 | 170.4 | 169.3 | 170.3 | # | 170.2 | 171.5 | # |
| 25 | 34.8 | 34.8 | 39.3 | 35.3 | 35.4 | 35.6 | 35.7 | 32.8 | 35.6 | 35.8 | 35.3 | 35.3 | 35.7 | 35.4 | 35.6 |
| 26 | 23.8 | 31.7 | 22.9 | 30.4 | 26.4 | 23.7 | 30.7 | 23.8 | 22.6 | 30.3 | 25.4 | 30.2 | 24.3 | 23.5 | 30.2 |
| 27 | 23.3 | 29.3 | 33.0 | 23.5 | 24.1 | 33.5 | 23.8 | 23.4 | 33.1 | 23.8 | 25.3 | 23.0 | 23.9 | 33.0 | 23.2 |
| 28 | 14.6 | 14.6 | 22.9 | 32.4 | 14.3 | 23.7 | 32.9 | 14.0 | 23.5 | 32.4 | 14.3 | 32.5 | 14.1 | 23.0 | 32.4 |
| 29[k] | — | 22.5[k] | 14.2 | 22.6 | — | 14.2 | 23.8 | — | 14.4 | 23.8 | — | 23.0 | — | 14.0 | 23.2 |
| 30 | — | | — | 14.3 | — | — | 14.2 | — | — | 14.3 | — | 14.1 | — | — | 14.1 |
| 4-Me | 15.0 | 15.0 | 14.9 | 15.1 | 14.8 | 14.9 | 15.0 | 15.0 | 15.4 | 15.0 | 15.4 | 14.9 | 15.4 | 15.0 | 15.0 |
| 8-Me | 12.5 | 12.5 | 12.9 | 12.8 | 12.6 | 12.6 | 12.6 | 12.8 | 13.2 | 12.6 | 13.2 | 12.8 | 13.2 | 12.9 | 12.7 |
| 12-Me | 17.5 | 17.5 | 17.2 | 17.8 | 18.1 | 18.1 | 18.0 | 17.7 | 18.2 | 17.8 | 18.1 | 17.8 | 18.1 | 17.8 | 17.7 |
| 22-Me | 14.3 | 14.3 | 14.4 | 14.5 | 13.7 | 13.8 | 13.7 | 14.4 | 14.8 | 14.3 | 14.8 | 14.5 | 14.3 | 14.5 | 14.4 |
| 1′ | 173.8[a] | 173.1[b] | 173.2[c] | 172.9[d] | 172.7[e] | 172.9[f] | 173.4[g] | 176.9 | 173.3 | 174.0 | 165.9[h] | 165.2[i] | 162.7[j] | # | # |
| 2′ | 30.9 | 29.8 | 31.3 | 31.1 | 30.0 | 30.3 | 30.1 | 30.9 | 31.2 | 30.9 | 135.7 | 134.9 | 147.8 | 148.2 | 147.8 |
| 3′ | 29.7 | 30.9 | 29.7 | 29.7 | 29.8 | 29.6 | 29.6 | 29.6 | 29.9 | 29.5 | 135.7 | 134.9 | 117.8 | 117.2 | 117.4 |
| 4′ | 176.4[a] | 175.6[b] | 175.8[c] | 175.4[d] | 175.7[e] | 175.9[f] | 176.0[g] | 174.4 | 174.7 | 174.2 | 169.4[h] | 168.1[i] | 123.4 | 123.6 | 123.1 |
| 5′ | — | | — | — | — | — | — | — | — | — | — | — | 152.2 | 151.3 | 152.1 |
| 6′ | — | | — | — | — | — | — | — | — | — | — | — | 161.1[j] | # | # |
| $CO_2Me$ | — | | — | — | — | — | — | 51.8 | 52.4 | 51.9 | — | — | — | — | — |

[a–j] Assignments interchangeable. [k] Pos. 29 refers to 27-Me in reveromycin C (**3**). # Not observed.

of the structure elucidation of the full suite of reveromycins isolated from *Streptomyces* spp. MST-MA568 and MST-RA7781 is shown below.

### Reveromycin hemi-succinates

The HRESI(+)MS data for **1** revealed a pseudomolecular ion $(M+Na)^+$ corresponding to a molecular formula ($C_{36}H_{52}O_{11}$, Δmmu −1.6) requiring eleven double bond equivalents (DBE). The 1D and 2D NMR (MeOH-$d_4$) data for **1** (Table 1 and Table S1, ESI†), together with UV-Vis and $[\alpha]_D$ data, were in good agreement with those previously reported for the 6,6-spiroketal reveromycin A (Fig. 2).[4] More specifically, as illustrated in Fig. 3, key 2D NMR correlations established the planar structure for reveromycin A, while $^1H$–$^1H$ coupling constants and $^{13}C$ chemical shifts defined geometry about $\Delta^{2,3}$, $\Delta^{6,7}$, $\Delta^{8,9}$, $\Delta^{20,21}$ and $\Delta^{22,23}$. Of particular note, the $^{13}C$ NMR chemical shifts for C-15 ($\delta_C$ 97.1) and C-18 ($\delta_C$ 84.2), and $^1H$ NMR resonance for H-19 ($\delta_H$ 4.63), proved diagnostic for the 6,6-spiroketal reveromycin A *vs.* the 5,6-spiroketal reveromycin B (C-15, $\delta_C$ 108.7; C-18, $\delta_C$ 88.5; H-19, $\delta_H$ 5.56), while the C-18 *n*-butyl sidechain was characterized by NMR shifts across C-25 to C-28 (Table 1) and $H_3$-28 ($\delta_H$ 0.86, t, *J* 6.7 Hz) (Table S1, ESI†).

The HRESI(+)MS data for **2** revealed a pseudomolecular ion $(M+Na)^+$ corresponding to a molecular formula ($C_{36}H_{52}O_{11}$, Δmmu −0.5) isomeric with **1**, with 1D and 2D NMR (MeOH-$d_4$) data (Table 1 and Table S2, ESI†) in good agreement with those previously reported for the 5,6-spiroketal reveromycin B.[4] As illustrated in Fig. 3, key 1D and 2D NMR resonances and correlations established the planar structure for the 5,6-spiroketal reveromycin B and C-18 *n*-butyl sidechain ($\delta_C$ 35.4, 26.4, 24.1 and 14.3; $H_2$-28, $\delta_H$ 0.92, t, *J* 6.9 Hz), while $^1H$–$^1H$ coupling constants and $^{13}C$ chemical shifts defined geometry about $\Delta^{2,3}$, $\Delta^{6,7}$, $\Delta^{8,9}$, $\Delta^{20,21}$ and $\Delta^{22,23}$. As the absolute configurations of **1** and **2** had previously been established through degradation and synthesis (see above), all the spiroketal reveromycin co-metabolites of **1** and

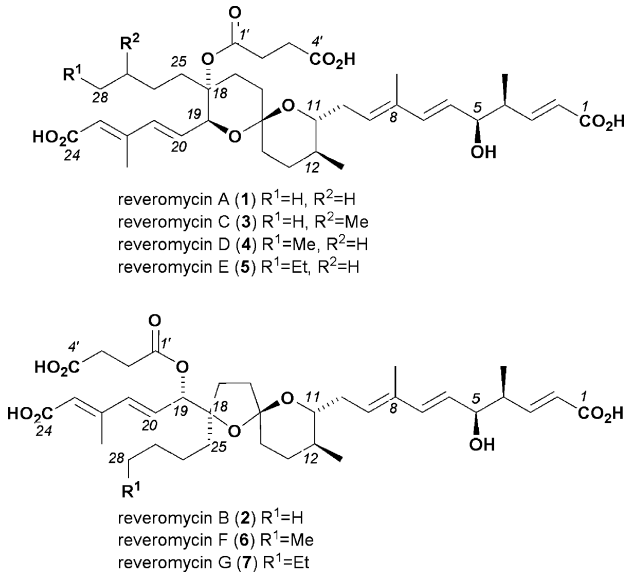


**Fig. 2** Reveromycin hemi-succinates **1–7**.

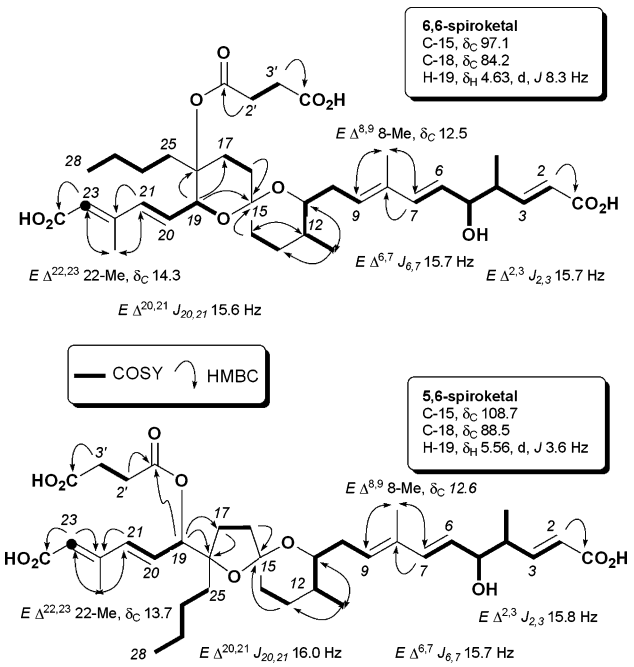


**Fig. 3** Key 2D NMR (MeOH-$d_4$) correlations for the 6,6-spiroketal (**1**), and 5,6-spiroketal (**2**) reveromycins.

**2** described below were attributed the same absolute configuration on biogenetic grounds.

The HRESI(+)MS data for **3** and **4** revealed pseudomolecular ions $(M+Na)^+$ corresponding to a molecular formula ($C_{37}H_{54}O_{11}$, Δmmu –0.9 and –2.2 respectively) for higher ($CH_2$) homologues of **1**. The 1D and 2D NMR (MeOH-$d_4$) data for **3** and **4** (Table 1 and Tables S3 and S4, ESI†) indicated 6,6-spiroketals with an isopentyl and *n*-pentyl C-18 alkyl side chains respectively, consistent with the known 6,6-spiroketals reveromycins C and D.[4]

The HRESI(–)MS data for **5** revealed a pseudomolecular ion $(M–H)^-$ corresponding to a molecular formula ($C_{38}H_{56}O_{11}$, Δmmu –1.8) for a higher ($CH_2$) homologue of **4**. The 1D and 2D NMR (MeOH-$d_4$) data for **5** (Table 1 and Table S5, ESI†) indicated a 6,6-spiroketal with an *n*-hexyl C-18 alkyl side chain, consistent with a new 6,6-spiroketal polyketide, reveromycin E (**5**).

The HRESI(+)MS data for **6** and **7** revealed pseudomolecular ions $(M+Na)^+$ corresponding to molecular formulae ($C_{37}H_{54}O_{11}$, Δmmu –1.5 and $C_{38}H_{56}O_{11}$, Δmmu –3.3) consistent with higher ($CH_2$ and $CH_2CH_2$) homologues of **2**. The 1D and 2D NMR (MeOH-$d_4$) data for **6** (Table 1 and Table S6, ESI†) and **7** (Table 1 and Table S7, ESI†) indicated 5,6-spiroketals with *n*-pentyl and *n*-hexyl C-18 alkyl side chains respectively, consistent with the new 5,6-spiroketal polyketide, reveromycins F (**6**) and G (**7**).

### Reveromycin 4′-methyl esters

The HRESI(+)MS data for **8** revealed a pseudomolecular ion $(M+Na)^+$ corresponding to a molecular formula ($C_{37}H_{54}O_{11}$, Δmmu –2.1) consistent with a methyl ester of **1**. The 1D and 2D NMR (MeOH-$d_4$) data for **8** (Table 1 and Table S8, ESI†) indicated a 6,6-spiroketal with an *n*-butyl C-18 alkyl side chain. The only significant difference in the NMR data between **8** and **1** was the appearance of a methyl ester resonance ($\delta_H$ 3.68, s; $\delta_C$ 51.8) with an HMBC correlation to C-4′ of the succinate residue, consistent with a new 6,6-spiroketal polyketide, reveromycin A 4′-methyl ester (**8**) (Fig. 4).

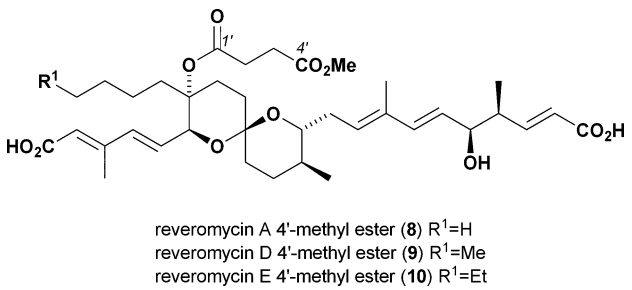


**Fig. 4** Reveromycin 4′-methyl esters **8–10**.

The HRESI(+)MS data for **9** and **10** revealed pseudomolecular ions [$(M+Na)^+$ and $(M–H)^-$ respectively] corresponding to molecular formulae ($C_{38}H_{56}O_{11}$, Δmmu –1.3 and $C_{39}H_{58}O_{11}$, Δmmu –1.3) consistent with methyl esters of **4** and **5**. The 1D and 2D NMR (MeOH-$d_4$) data for **9** (Table 1 and Table S9, ESI†) and **10** (Table 1 and Table S10, ESI†) indicated 6,6-spiroketals with *n*-pentyl and *n*-hexyl C-18 alkyl side chains, respectively. The only significant differences in the NMR data between **9** and **4**, and **10** and **5**, were the appearance of methyl ester resonances (**9**; $\delta_H$ 3.68, s; $\delta_C$ 52.4; **10**; $\delta_H$ 3.68, s; $\delta_C$ 51.9) with HMBC correlations to C-4′ of the succinate residue, consistent with the new 6,6-spiroketal polyketides reveromycin D 4′-methyl ester (**9**) and reveromycin E 4′-methyl ester (**10**).

### Reveromycin hemi-fumarates

The HRESI(+)MS data for **11** revealed a pseudomolecular ion $(M+Na)^+$ corresponding to a molecular formula ($C_{36}H_{50}O_{11}$, Δmmu –0.5) consistent with a di-dehydro analogue of **1**. The 1D and 2D NMR (MeOH-$d_4$) data for **11** (Table 1 and Table S11, ESI†) indicated a 6,6-spiroketal with an *n*-butyl C-18 alkyl side chain. The only significant differences in the NMR data between **11** and **1** were replacement of resonances and correlations for the hemi-succinate residue with those for an *E*-hemi-fumarate ($\delta_H$

 

6.78, $AB_q$, $J_{2',3'}$ 15.7 Hz, H-2′ and H-3′; $\delta_C$ 135.7, C-2′ and C-3′; 165.9/169.4, C-1′/C-4′), consistent with a new 6,6-spiroketal polyketide, reveromycin H (**11**) (Fig. 5). The HRESI(+)MS data for **13** revealed a pseudomolecular ion $(M+Na)^+$ corresponding to a molecular formula ($C_{38}H_{54}O_{11}$, Δmmu −2.5) for a higher ($CH_2CH_2$) homologue of **11**. The 1D and 2D NMR (MeOH-$d_4$) data for **13** (Table 1 and Table S13, ESI†) indicated a 6,6-spiroketal with an *n*-hexyl C-18 alkyl side chain, and an *E*-hemi-fumarate ($\delta_H$ 6.78, $AB_q$, $J_{2',3'}$ 15.8 Hz, H-2′ and H-3′; $\delta_C$ 134.9, C-2′ and C-3′; 165.2/168.1, C-1′/C-4′) consistent with a new 6,6-spiroketal polyketide, reveromycin J (**13**), as shown. The *E*-hemi-fumarate reveromycin I (**12**) was not isolated and independently characterized, but was nevertheless detected during analytical profiling (discussed later).

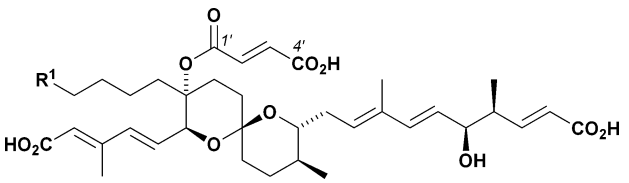


reveromycin H (**11**) $R^1$=H
reveromycin I (**12**) $R^1$=Me
reveromycin J (**13**) $R^1$=Et

**Fig. 5** Reveromycin hemi-fumarates **11–13**.

### Reveromycin hemi-furanoates

The HRESI(–)MS data for **14** revealed a pseudomolecular ion $(M–H)^-$ corresponding to a molecular formula ($C_{38}H_{50}O_{12}$, Δmmu −2.5) requiring fourteen DBE. The 1D and 2D NMR (MeOH-$d_4$) data for **14** (Table 1 and Table S14, ESI†) indicated a 6,6-spiroketal with an *n*-butyl C-18 alkyl side chain. The only significant differences in the NMR data between **14** and **1** were replacement of resonances and correlations for the hemi-succinate with an alternative ester, incorporating two trisubstituted oxo-olefins ($\delta_H$ 7.44, H-3′, $\delta_C$ 147.8, C-2′, $\delta_C$ 117.8, C-3′; and $\delta_H$ 8.36, H-5′, $\delta_C$ 123.4, C-4′, $\delta_C$ 152.2, C-5′). The analysis presented above accounts for $C_{36}H_{49}O_9$ and eleven DBE (the reveromycin A polyketide framework, less the hemi-succinate but inclusive of two trisubstituted oxo-olefins bearing a common oxygen). The remaining elements ($C_2HO_3$ and three DBE) were attributed to a carbonyl (to complete the C-18 ester linkage) and a carboxylic acid ($CO_2H$), with the final DBE accommodated by a furan ring—consistent with a C-18 hemi-furanoate of a furan dicarboxylic acid. Comparison of the $^1H$ NMR chemical shifts for the furan methines H-3′ and H-5′ with those reported for synthetic 2,3- ($CDCl_3$, $\delta_H$ 6.73 and 7.48)[15] and 2,4- (DMSO-$d_6$, $\delta_H$ 7.40 and 8.54)[16] furan dicarboxylate esters, suggested that **14** incorporates a 2,4-furan dicarboxylic acid.

To complete the structure elucidation of **14**, determination of the regiochemistry of the C-18 hemi-furanoate ester linkage was required. The lack of diagnostic 2D NMR correlations linking the furanoate functionality to the core polyketide skeleton in **14** (or its synthetic trimethylated derivative **14a**) precluded a direct assignment of regiochemistry. In an attempt to resolve this structural feature, we compared experimental NMR (MeOH-$d_4$) chemical shifts for H-5′ in **14**, and H-5′ and C-6′ in **14a**, with predicted values (ACD software) for the two alternate regiochemistries, subunits A and B (see Fig. 6). This analysis favoured assignment of the subunit B regiochemistry to **14** and **14a**, and permitted structure assignment of a new 6,6-spiroketal polyketide, reveromycin K (**14**), featuring an unprecedented hemi-furanoate functionality (Fig. 7).

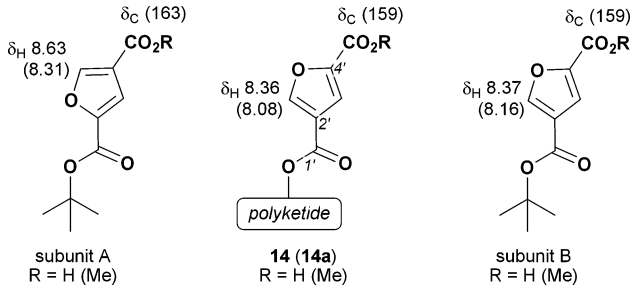


**Fig. 6** Reveromycin hemi-furanoate regiochemistry.

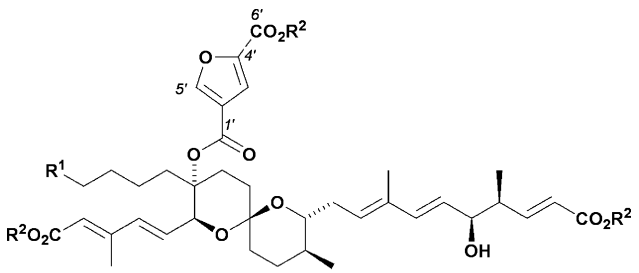


reveromycin K (**14**) $R^1$=H, $R^2$=H
reveromycin K trimethyl ester (**14a**) $R^1$=H, $R^2$=Me
reveromycin L (**15**) $R^1$=Me, $R^2$=H
reveromycin M (**16**) $R^1$=Et, $R^2$=H

**Fig. 7** Reveromycin hemi-furanoates **14–16**.

The HRESI(–)MS data for **15** and **16** revealed pseudomolecular ions [$(M–H)^-$ and $(M+Na)^+$ respectively] corresponding to molecular formulae ($C_{39}H_{52}O_{12}$, Δmmu −2.7 and $C_{40}H_{54}O_{12}$, Δmmu −1.8) consistent with homologues ($CH_2$ and $CH_2CH_2$) of **14**. The 1D and 2D NMR (MeOH-$d_4$) data for **15** (Table 1 and Table S15, ESI†) and **16** (Table 1 and Table S16, ESI†) indicated 6,6-spiroketals with *n*-pentyl and *n*-hexyl C-18 alkyl side chains respectively, consistent with the new 6,6-spiroketal polyketides, reveromycin L (**15**) and reveromycin M (**16**).

### Analytical profiling

An examination of the suite of reveromycin co-metabolites isolated during this investigation revealed a noteworthy pattern in which the three 6,6-spiroketal hemi-succinates **1**, **4** and **5** were matched with (a) three 5,6-spiroketal hemi-succinates **2**, **6** and **7**, (b) three 6,6-spiroketal hemi-succinate 4′-methyl esters **8**, **9** and **10**, and (c) three 6,6-spiroketal hemi-furanoates **14**, **15** and **16**, but only (d) two 6,6-spiroketal hemi-fumarates **11** and **13**. As the isolation of reveromycins from the highly complex *Streptomyces* sp. MST-RA7781 extract was a major technical challenge, it was reasonable to assume that the "missing" member of the hemi-fumarate homologous series, reveromycin I (**12**), was a co-metabolite that

eluded efforts at isolation and characterization by HPLC-DAD-SPE-NMR. In an attempt to confirm this hypothesis, and detect the "missing" reveromycin I (**12**), we turned our attention to the HPLC-DAD-MS data acquired on the crude extract of *Streptomyces* sp. MST-RA7781 (Fig. 8). Although direct interpretation of the complex total ion chromatogram was clearly problematic, selective ion monitoring proved particularly informative. For example, extracted ion chromatograms (supported by direct comparison to authentic standards) clearly revealed the set of hemi-furanoates, reveromycins K (**14**) (*m*/*z* 697), L (**15**) (*m*/*z* 711) and M (**16**) (*m*/*z* 725). By comparison, extracted ion chromatograms for the hemi-fumarates, reveromycins H (**11**) (*m*/*z* 657), I (**12**) (*m*/*z* 671) and J (**13**) (*m*/*z* 685), revealed three well resolved peaks, with authentic standards confirming the identity of leading and trailing peaks as **11** and **13** respectively. Significantly, an overlay of these two chromatograms highlighted a common pattern of both relative abundance and relative retention time—revealing a peak at the anticipated retention time, and with HRESI(–)MS and UV-Vis spectra consistent with those expected for **12**. While not formally isolated, on the basis of the analyses outlined above, we suggest that **12** is a *Streptomyces* sp. MST-RA7781 metabolite.

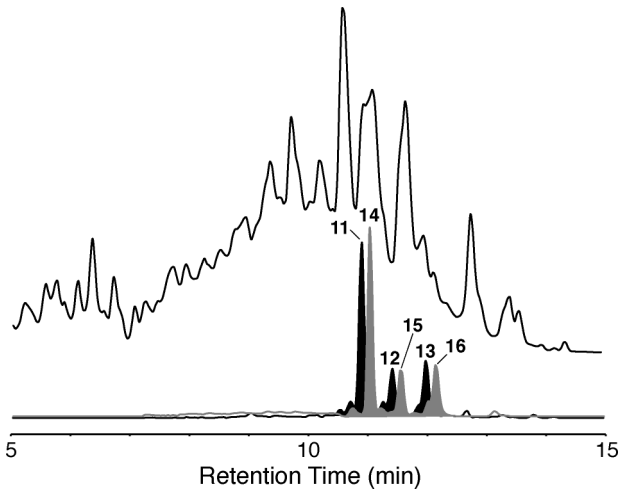


**Fig. 8** Unshaded: HPLC-ESI(–)MS total ion chromatogram of a crude extract from *Streptomyces* sp. MST-RA7781. Black shading: Selected ion chromatogram (*m*/*z* 697, 711, 725) corresponding to the homologous series of hemi-furanoate reveromycins K–M (**14–16**) respectively. Grey shading: Selected ion chromatogram (*m*/*z* 657, 671, 685) corresponding to the homologous series of hemi-fumarate reveromycins H–J (**11–13**) respectively.

### Hemi-succinyl : ketal-succinyl equilibria

During HPLC purification and analysis of the reveromycins, we were intrigued to consistently observe the presence of minor later-eluting "contaminant" peaks (**1***, **3***, **4*** and **5***) in each of the supposedly pure samples of the hemi-succinate reveromycins A (**1**), C (**3**), D (**4**) and E (**5**), but not for any of the other reveromycins **6–16**. Using **1** as a case study (Fig. 9), we employed: (i) HPLC-DAD-MS analysis to establish that **1** and **1*** were isomeric; (ii) HPLC-DAD-SPE-NMR analysis to establish that $^1$H NMR spectra for **1** and **1*** were essentially identical; (iii) semi-preparative HPLC

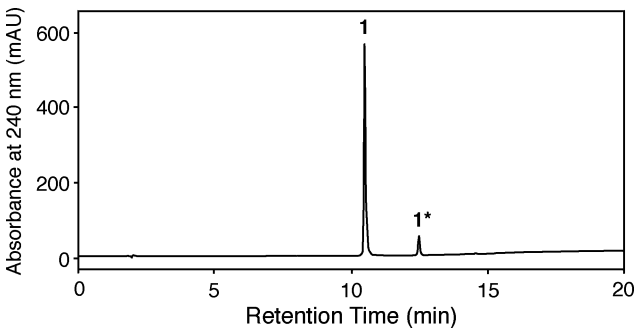


**Fig. 9** HPLC-DAD chromatogram (240 nm) of purified reveromycin A (**1**) showing trace levels of the cyclized ketal-succinyl species (**1***).

to fractionate **1** and **1*** and establish by a time course HPLC-DAD analysis, an equilibrium relationship. In this latter study, freshly separated samples of **1** and **1*** were stored immediately post fractionation at 30 °C in HPLC eluant ($H_2O$–MeCN), in collection vials within the HPLC fraction collector, where they were observed to undergo equilibration over a period of 24 h to re-establish a final **1** : **1*** ratio of 85 : 15. [Note: The ratio of parent to equilibrium species (*e.g.* **1** : **1***) varied across the hemi-succinates **1**, **3–5** and also with the HPLC method of analysis (*i.e.* column bonded phase, solvent, pH) from ~85 : 15 to ~99 : 1].

In an effort to explain these observations, we hypothesized that the hemi-succinate moiety in **1** (and related co-metabolites **3–5**) underwent intramolecular cyclization to establish an equilibrium with the ketal-succinyl species (**1***) (Fig. 10). By contrast, the co-metabolite hemi-succinate 4′-methyl esters (**8–10**), hemi-fumarates (**11–13**) and hemi-furanoates (**14–16**) were incapable of forming a ketal-succinyl and as such did not equilibrate—explaining the lack of "contaminant" peaks during HPLC analysis. The reason why the 5,6-spiroketal reveromycins **2**, **6** and **7** failed to undergo a ketal-succinyl equilibrium was less obvious and required a more detailed mechanistic consideration of the behaviour of hemi-succinates.

In building this mechanistic model, we reviewed the scientific literature and noted that, while well known across natural and synthetic chemistry, hemi-succinates had not previously been observed to equilibrate to ketal-succinyl species. Thus, for our proposed reveromycin ketal-succinyl hypothesis to have merit would require that hemi-succinyl reveromycins possess unique structural characteristics that facilitate (stabilize) this equilibrium. We were encouraged that this may be the case by noting that hemi-succinyl reveromycins are the only known examples of 6,6-spiroketals bearing a pendant hemi-succinate. Following this line of reasoning, we hypothesized that the ketal-succinyl was stabilized by a seven-membered hydrogen bonded ring, linking the ketal-succinyl 1′-OH and the 6,6-spiroketal (Fig. 10). This hypothesis has the dual merits of explaining both (a) the unique ability of 6,6-spiroketal reveromycin hemi-succinates to equilibrate to ketal-succinyl species, and (b) the inability of 5,6-spiroketal reveromycins hemi-succinates to achieve a comparable equilibrium, as the latter compounds cannot form a suitably stablized seven-membered hydrogen bonded ring system. While the discussion presented above provides a plausible theoretical explanation for what, at first glance, may appear to be a relatively inconsequential experimental anomaly (minor HPLC contaminant), on closer reflection this analysis assumed greater significance.

 

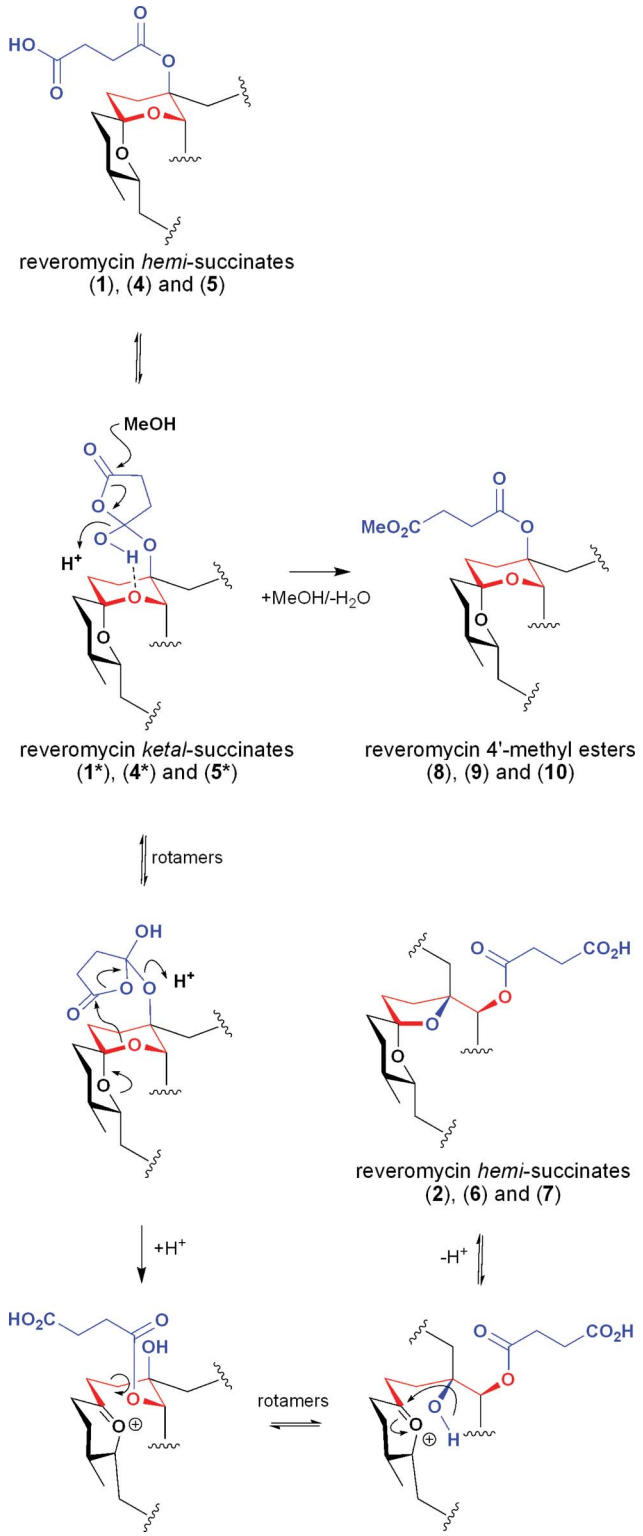


**Fig. 10** Hemi-succinyl : ketal-succinyl equilibrium as a mechanism for the formation of 4′-methyl ester and 5,6-spiroketal artifacts.

### Natural products or artifacts?

The use of MeOH during the extraction, fractionation and handling of natural product carboxylic acids brings with it the risk of methyl ester artifacts, a risk that is further amplified in the case of the tricarboxylic acid reveromycins. This risk notwithstanding, in this current study the discovery of methyl esters was curiously restricted to the 4′-methyl esters **8–10** (and not 1- or 24- methyl esters). Such selectivity would normally be indicative of biosynthetic intervention and would be taken as evidence that **8–10** were natural products and not artifacts. However, in light of the ketal-succinyl equilibrium elaborated above, we were alert to another possibility. As illustrated in Fig. 10, the ketal-succinyl residue is primed for nucleophilic attack, which if achieved by the solvent MeOH could explain the selective formation of 4′-methyl esters. Furthermore, as the ketal-succinyl equilibrium is limited to the 6,6-spiroketal hemi-succinates, and not the hemi-fumarates **11–13**, hemi-furanoates **14–16** or the 5,6-spiroketal hemi-succinates **2**, **6** and **7**, this explains the restricted distribution of isolated reveromycin methyl esters. Building on the ketal-succinyl equilibrium hypothesis and the selected structural diversity of isolated reveromycins, the arguments outlined above support the proposition that **8–10** are artifacts, not natural products.

Encouraged by the ability of the ketal-succinyl equilibrium to explain the formation of reveromycin 4′-methyl ester artifacts, we turned our attention to reveromycin 5,6-spiroketals. With a wide array of reveromycins for comparison, we were initially surprised that the distribution of reveromycin 5,6-spiroketals was restricted exclusively to hemi-succinates (**2**, **6** and **7**), with no evidence of 4′-methyl esters, hemi-fumarates or hemi-furanoates. This distribution pattern suggested that the reveromycin 5,6-spiroketals were artifacts of the 6,6-spiroketal hemi-succinates, mediated by the ketal-succinyl equilibrium.

Before developing this argument further, it is worthwhile pausing to note that the current scientific literature on reveromycin biosynthesis is limited to the simple observation that "reveromycins are polyketides"—being silent on the specifics of the biosynthetic pathway, let alone any possible relationship between 6,6- and 5,6-spiroketals. Putting this lack of biosynthetic detail to one side, the synthetic literature is more forthcoming. Synthetic chemists have noted that reveromycin 6,6-spiroketal intermediates lacking the hemi-succinate residue (but bearing an 18-OH moiety) are prone to ring contraction to 5,6-spiroketals. In fact, avoiding this ring contraction was a significant technical achievement in the syntheses of reveromycin A (**1**). Implicit in these synthetic accounts is the unstated view that the hemi-succinate residue acts as a molecular lock, trapping natural 6,6-spiroketals, preventing spiroketal ring contraction to more stable 5,6-spiroketals, and affirming that the 5,6-spiroketals are natural products.

Notwithstanding the logic of these arguments, based as they were on the available data, the proposed ketal-succinyl equilibrium raises the possibility of a rearrangement pathway directly linking the natural 6,6-spiroketal reveromycin hemi-succinates to their 5,6-spiroketal isomers. That this can be achieved without the requirement for hemi-succinate hydrolysis (Fig. 10) brings into question the biosynthetic origins of the 5,6-spiroketal reveromycins. As illustrated in Fig. 10, the ketal-succinyl equilibrium allows for rotation of the ketal-succinyl residue to bring the activated carbonyl into the proximity of the core 6,6-spiroketal system. In a subsequent concerted sequence of events, the 6,6-spiroketal can undergo ring opening, initiating a *trans*-esterification that culminates in 5,6-spiroketal ring closure. Such a mechanism provides a plausible pathway from 6,6- to 5,6-spiroketals that fully explains

the requirement for a hemi-succinate residue and the limited distribution of 5,6-spiroketal diversity. Although hypothetical, if such a transformation could be performed under conditions comparable to those encountered during extraction, fractionation and/or handling, the reveromycin 5,6-spiroketals would best be redefined as artifacts. To test this hypothesis, we maintained a sample of reveromycin A (**1**) in a solution of $H_2O$–MeCN (1 : 1) at 60 °C for 4 d, generating a complex mixture from which we isolated reveromycin B (**2**) (identical in all respects to an authentic sample). This study provides a theoretical and experimental basis to conclude that the reveromycin 5,6-spiroketals **2**, **6** and **7** are, in all probability, artifacts.

It is worthwhile noting that while many chemists perceive artifacts derived from natural products in a negative light, judging them to be failures or mistakes of the isolation process and as such of lesser or even no importance, this downgrading of the value of artifacts has significant consequences. For example, whereas synthetic chemists are eager to take up the challenge of preparing natural products, few view artifacts as worthy targets (unless, as in the case of reveromycin B, the artifact status emerges unexpectedly at a later date). Similarly, natural product chemists can be dismissive of efforts expended in describing "mere" artifacts, perpetuating a prejudice that clouds and even discourages a willingness to decipher the story artifacts have to tell. That selected natural products are "primed" to undergo chemical transformations leading to artifacts, without the intervention of enzymes, demonstrates an ability to access extended new chemical space without genetic overhead—surely a good thing from an evolutionary (and potentially pharmacological) perspective. Artifacts should be valued for what they reveal, not relegated to footnotes because they lack some notional sense of purity of enzymatic lineage reserved for natural products.

## Biosynthesis

Having identified which of the reveromycins encountered in this study were not natural products, we next turned our attention to consider the reveromycin polyketide biosynthesis. Fig. 11 provides a schematic representation of a plausible reveromycin polyketide biosynthesis. This proposed biosynthetic pathway has three noteworthy features: (i) a 2-methylsuccinyl-CoA starter residue; (ii) flexibility to incorporate a selection of pre-formed $C_{6\text{-}8}$ polyketide residues to account for the range of C-18 sidechains (*n*-butyl, *n*-pentyl, *n*-hexyl and *n*-isohexyl); (iii) coordinated but flexible delivery of a selection of succinate, fumarate and furanoate moieties to account for the range of ester residues. While this biosynthetic proposal remains untested experimentally, it does nevertheless satisfy key considerations and raises a number of interesting prospects. Firstly, as *Streptomyces* isolates capable of high level reveromycin production are exceptionally rare (in

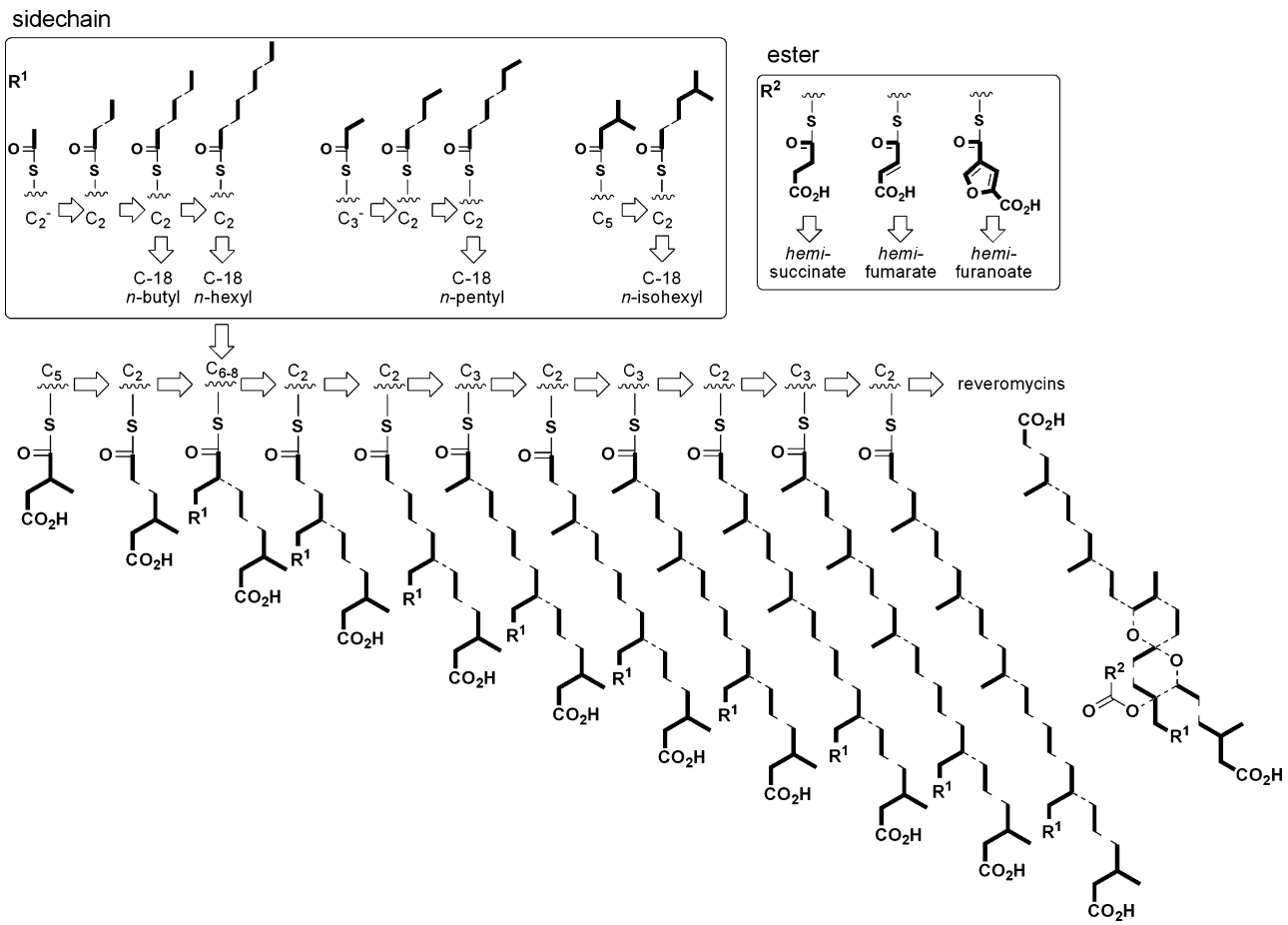


**Fig. 11** Plausible reveromycin polyketide biosynthesis.

 

our collection only 1 out of 400 000), the proposed biosynthesis suggests the option to supplement culture media with 2-methylsuccinic acid as a possible means to increase production levels. Furthermore, as recent precursor-directed biosynthetic investigations into the polyketide borrelidin have demonstrated[17] cross over starter unit substrate specificity between (1*R*,2*R*)-cyclopentane-1,2-dicarboxylic acid and 2-methylsuccinic acid, the former may represent an excellent culture media supplement to generate new unnatural reveromycin analogues. Secondly, as reveromycin ester residues are limited to a set of three structurally related dicarboxylic acids (succinic, fumaric and furandicarboxylic), this suggests that incorporation is guided by a diacid acyl carrier protein (ACP) with a defined but nevertheless moderately flexible substrate specificity. Supplementation of culture media with alternative carboxylic acids (*e.g.* furan-2-carboxylic acid, *Z*-fumaric acid, cyclopentane-1,2-dicarboxylic acid) may facilitate production of new unnatural reveromycin esters. Thirdly, use of an unnatural substrate to inhibit the diacid ACP complex could have the effect of diverting polyketide output from the reveromycin to spirofungin structure class. The spirofungins are closely related polyketides reported in 1998 from an Australian soil actinomycete *Streptomyces violaceusniger*[18] and have promising antifungal activity. Also, in common with the reveromycins, further development of the spirofungin motif is hampered by restricted access to both material and suitable analogues. Finally, directed and/or random mutation of the *Streptomyces* sp. MST-MA568 and/or *Streptomyces* sp. MST-RA7781 polyketide synthase could provide an exciting entry into new and diverse reveromycins. The approaches outlined above, building on the proposed reveromycin polyketide biosynthsis, provide attractive strategies for accessing new reveromycins that could in turn be used to further probe biological activity.

### Biological Activity

Literature accounts of the anticancer properties of reveromycins acknowledge the anti-proliferative activity of **1**, **3** and **4** against KB (human oral) and K562 (human leukemia) cell lines ($IC_{50}$ ~3 μM)[3] (Note: the KB cell line has since been reclassified as a HeLa variant[19]), and note **1** as a cell cycle inhibitor targeting Ile t-RNA synthetase ($IC_{50}$ 2 nM),[14,20] with potential value in the treatment of osteolytic bone metastasis of osteoporosis[20] and lung cancer.[21] In our hands, selected reveromycins displayed only modest cytotoxicity against a selection of human cell lines (Table S17, ESI†), with the 4′-methyl esters **8** and **9** being notably cytotoxic to AGS (stomach) and HeLa (cervical) ($IC_{50}$ 2–10 μM), but not HT29 (colon) and HFF-1 (fibroblast) ($IC_{50}$ >30 μM) cell lines. No significant antibacterial activity was observed against *Escherichia coli* (ATCC 11775), *Pseudomonas aeruginosa* (ATCC 10145), *Staphylococcus aureus* (ATCC 9144, ATCC 25923) or *Bacillus subtilis* (ATCC 6051, ATCC 6633).

While not antibacterial, reveromycins **1**, **3** and **4** have previously been described as antifungal against *Candida albicans*, with an *in vitro* MIC superior to that of the commercial antifungal agent fluconazole at pH 3.[3] Our investigations confirm these findings (Table S18, ESI†), and go on to note a 2–4 fold improvement in antifungal activity for the 4′-methyl esters (**8** and **9**) against *C. albicans* (ATCC 10231), *C. krusei* (ATCC 6258) and *C. parapsilosis* (ATCC 22019) at pH 3. The hemi-furanoates (**13–15**) showed a 2–4 fold decrease in antifungal activity, while the 5,6-spiroketals (**2**, **6** and **7**) showed no appreciable activity.

## Conclusions

Our investigations into two Australian *Streptomyces* spp. have substantially advanced knowledge of the rare reveromycin class of polyketide spiroketals, providing a comprehensive spectroscopic data set and increasing the number of known natural reveromycins from four to sixteen. In the process of investigating these metabolites, we showcased HPLC-DAD-SPE-NMR and HPLC-DAD-MS as powerful tools to resolve complex natural extracts that defy traditional methods. Armed with a large array of "isolated" reveromycins, we described an unprecedented hemi-succinate : ketal-succinyl equilibrium phenomenon and use mechanistic knowledge to build the case that the reveromycin 4′-methyl esters and the reveromycin 5,6-spiroketals are artifacts. We proposed a plausible polyketide biosynthesis consistent with expanded knowledge of reveromycin diversity and chemistry, and use this to provide informed commentary on possible strategies for further increasing and diversifying reveromycin production. Finally, we extended structure activity relationship investigations (SAR by co-metabolite) across the reveromycins, to assess anticancer, antibacterial and antifungal properties.

## Experimental

### General Experimental Details

General experimental details are given in the ESI.†

### Collection and Taxonomy

MST-MA568 was isolated from a sediment sample collected in 1997 near Nelson in the Glenelg River region of South Australia, during a study directed at marine-derived actinomycetes. Analysis of the 16S rRNA gene sequence revealed the organism to be a *Streptomyces* sp. (see ESI†). MST-RA7781 was isolated from a soil sample collected near Temora, New South Wales, Australia, during a study directed at rare actinomycetes. Analysis of the 16S rRNA gene sequence revealed the organism to be a *Streptomyces* sp. (see ESI†).

### Cultivation and Fractionation

Scaled-up production of metabolites from MST-MA568 was achieved *via* a citrate ISP2 liquid fermentation (0.4% yeast extract, 1% malt extract, 0.4% glucose pH 7.3; 1 L; 28 °C, 5 d). The supernatant from this fermentation was dried *in vacuo* and was partitioned between $H_2O$ and *n*-BuOH. Gel chromatography (Sephadex LH-20, MeOH) and reversed phase HPLC (Zorbax RX-$C_8$, 250 × 9.4 mm, 5 μm, 2.2 mL $min^{-1}$, stepwise gradient elution comprising $H_2O$ (0.01% $NH_4OH$) for 10 min, ramping (2 min) to 90% $H_2O$–MeOH (0.01% $NH_4OH$) for 10 min, ramping (2 min) to 75% $H_2O$–MeOH (0.01% $NH_4OH$) for 10 min, ramping (2 min) to 10% $H_2O$–MeOH (0.01% $NH_4OH$) for 10 min) on the *n*-BuOH solubles returned samples of reveromycins A (**1**) and E (**5**) (Scheme S1, ESI†).

Scaled-up production of metabolites from MST-RA7781 was achieved *via* solid phase ISP2 cultivation. A cryo-preserved vial

of MST-RA7781 (2 mL) was thawed and streaked onto an ISP2 agar plate (0.4% yeast extract, 1% malt extract and 0.4% glucose with 2% bacteriological agar, pH 7.3) and incubated at 28 °C for 7 d. Agar plugs were used to inoculate a 250 mL unbaffled flask containing 50 mL of ISP2 media (as for above without the agar), which was shaken at 200 rpm for 3 d at 28 °C. Aliquots of the seed culture (20 × 2 mL) were mixed thoroughly with portions of autoclaved pearl barley (20 × 100 g) and the inoculated grain was dispensed into 15 cm glass Petri plates, which were incubated for 14 d at 28 °C. The grain was extracted with acetone (2 × 2.5 L) and the solvent was filtered through a fibreglass mat and evaporated to an aqueous concentrate (1.2 L) *in vacuo*. The aqueous concentrate was adjusted to pH 3 and extracted with ethyl acetate (2 × 1.5 L). The combined organic layer was reduced to dryness *in vacuo*, yielding 12 g of crude extract. A portion of the extract (5 g) was dissolved in methanol : DMSO (1 : 1) and fractionated by preparative HPLC (Phenomenex Luna $C_{18}$ column, 450 × 50 mm, 5 μm, 60 mL $min^{-1}$, isocratic elution with 50% MeCN–$H_2O$ + 0.01% trifluoroacetic acid over 30 min). Six fractions containing the major metabolites in the complex were collected and the MeCN was removed *in vacuo*. The aqueous residues were extracted with ethyl acetate (3 × 50 mL) and the combined organic layers were reduced to dryness under a stream of nitrogen to recover the enriched metabolites.

Two different technological approaches were used to purify and identify the reveromycins in the six crude fractions. A traditional semi-preparative HPLC strategy (Zorbax RX-$C_8$ column, 250 × 9.4 mm, 5 μm, 2.0 mL $min^{-1}$ using a range of $H_2O$–MeOH gradient elution profiles, both with and without addition of a 0.01% $NH_4OH$ modifier) succeeded in yielding reveromycins A (**1**), C (**3**), D (**4**), E (**5**) and E 4′-methyl ester (**10**) (Scheme S2, ESI†). An analytical HPLC-DAD-SPE-NMR and HPLC-DAD-MS strategy succeeded in identifying sixteen reveromycins (**1–16**) (Scheme S3, ESI†).

### Characterisation of Reveromycins

For $^1$H NMR spectra and tabulated 2D NMR data for the reveromycins, see Fig. S1–S16 and Tables S1–S16, ESI.† Percentage compositions were calculated relative to the parent crude acetone extract.

**Reveromycin A (1).** A white amorphous solid (15.6%). $[\alpha]_D^{20}$ –102 (*c* 0.13, MeOH). UV (MeOH) $\lambda_{max}$/nm (log ε) 239 (4.42), 248 (sh), 264 (sh) nm. ESI(±)MS (100 kV) *m/z* 683 $(M+Na)^+$, 659 $(M–H)^-$, 559 $(M–H–C_4H_4O_3)^-$; HRESI(+)MS *m/z* 683.3391 $(M+Na)^+$ (calcd for $C_{36}H_{52}O_{11}Na$, 683.3407).

**Reveromycin B (2).** A white amorphous solid (3.9%). ESI(±)MS (100 kV) *m/z* 683 $(M+Na)^+$, 659 $(M–H)^-$, 559 $(M–H–C_4H_4O_3)^-$. HRESI(+)MS *m/z* 683.3402 $(M+Na)^+$ (calcd for $C_{36}H_{52}O_{11}Na$, 683.3407).

**Reveromycin C (3).** A white amorphous solid (0.6%). $[\alpha]_D^{20}$ –109 (*c* 0.14, MeOH). ESI(±)MS (100 kV) *m/z* 697 $(M+Na)^+$, 673 $(M–H)^-$, 573 $(M–H–C_4H_4O_3)^-$. HRESI(+)MS *m/z* 697.3567 $(M+Na)^+$ (calcd for $C_{37}H_{54}O_{11}Na$, 697.3558).

**Reveromycin D (4).** A white amorphous solid (1.4%). $[\alpha]_D^{20}$ –116 (*c* 0.52, MeOH). UV (MeOH) $\lambda_{max}$/nm (log ε) 239 (4.59), 248 (sh), 266 (sh) nm. ESI(±)MS (100 kV) *m/z* 697 $(M+Na)^+$, 673 $(M–H)^-$, 573 $(M–H–C_4H_4O_3)^-$. HRESI(+)MS *m/z* 697.3542 $(M+Na)^+$ (calcd for $C_{37}H_{54}O_{11}Na$, 697.3564).

**Reveromycin E (5).** A white amorphous solid (7.5%). $[\alpha]_D^{20}$ –63 (*c* 0.010, MeOH). UV (MeOH) $\lambda_{max}$/nm (log ε) 236 (3.96), 249 (sh), 267 (sh) nm. ESI(±)MS (100 kV) *m/z* 711 $(M+Na)^+$, 687 $(M–H)^-$ 567 $(M–H–C_4H_4O_3)^-$. HRESI(–)MS *m/z* 687.3726 $(M–H)^-$ (calcd for $C_{38}H_{55}O_{11}$, 687.3744).

**Reveromycin F (6).** (2.2%). ESI(±)MS (100 kV) *m/z* 697 $(M+Na)^+$, 673 $(M–H)^-$ 574 $(M–H–C_4H_4O_3)^-$. HRESI(+)MS *m/z* 697.3549 $(M+Na)^+$ (calcd for $C_{37}H_{54}O_{11}Na$, 697.3564).

**Reveromycin G (7).** (1.9%). ESI(±)MS (100 kV) *m/z* 711 $(M+Na)^+$, 687 $(M–H)^-$ 587 $(M–H–C_4H_4O_3)^-$. HRESI(+)MS *m/z* 711.3687 $(M+Na)^+$ (calcd for $C_{38}H_{56}O_{11}Na$, 711.3720).

**Reveromycin A 4′-methyl ester (8).** (3.5%). ESI(±)MS (100 kV) *m/z* 697 $(M+Na)^+$, 673 $(M–H)^-$, 573 $(M–H–C_4H_4O_3)^-$. HRESI(+)MS *m/z* 697.3543 $(M+Na)^+$ (calcd for $C_{37}H_{54}O_{11}Na$, 697.3564).

**Reveromycin D 4′-methyl ester (9).** (0.5%). ESI(±)MS (100 kV) *m/z* 711 $(M+Na)^+$, 687 $(M–H)^-$. HRESI(+)MS *m/z* 711.3707 $(M+Na)^+$ (calcd for $C_{38}H_{56}O_{11}Na$, 711.3720).

**Reveromycin E 4′-methyl ester (10).** A white amorphous solid (1.7%). $[\alpha]_D^{20}$ –32 (*c* 0.015, MeOH). UV (MeOH) $\lambda_{max}$/nm (log ε) 231 (sh), 237 (4.74), 248 (sh) nm. ESI(±)MS (100 kV) *m/z* 725 $(M+Na)^+$, 701 $(M–H)^-$ 601 $(M–H–C_4H_4O_3)^-$. HRESI(–)MS *m/z* 701.3888 $(M–H)^-$ (calcd for $C_{39}H_{57}O_{11}$, 701.3901).

**Reveromycin H (11).** (4.3%). ESI(±)MS (100 kV) *m/z* 681 $(M+Na)^+$, 657 $(M–H)^-$ 557 $(M–H–C_4H_4O_3)^-$. HRESI(+)MS *m/z* 681.3246 $(M+Na)^+$ (calcd for $C_{36}H_{50}O_{11}Na$, 681.3251).

**Reveromycin I (12).** (not formally isolated). ESI(±)MS (100 kV) *m/z* 695 $(M+Na)^+$, 671 $(M–H)^-$, 571 $(M–H–C_4H_4O_3)^-$. HRESI(–)MS *m/z* 671.3436 $(M–H)^-$ (calcd for $C_{37}H_{51}O_{11}$, 671.3437).

**Reveromycin J (13).** (3.0%). ESI(±)MS (100 kV) *m/z* 709 $(M+Na)^+$, 685 $(M–H)^-$. HRESI(+)MS *m/z* 709.3539 $(M+Na)^+$ (calcd for $C_{38}H_{54}O_{11}Na$, 709.3564).

**Reveromycin K (14).** (5.3%). ESI(±)MS (100 kV) *m/z* 721 $(M+Na)^+$, 697 $(M–H)^-$. HRESI(–)MS *m/z* 697.3199 $(M–H)^-$ (calcd for $C_{38}H_{49}O_{12}$, 697.3224).

**Reveromycin K trimethyl ester (14a).** A solution of diazomethane in diethyl ether (0.08 M) was added dropwise to a solution of **14** (1.2 mg) in ethanol (3 mL) until a yellow colour persisted. The solution was then reduced to dryness under a stream of nitrogen, yielding **14a** as a white amorphous solid (1.3 mg, quant.). ESI(+)MS (60 kV) *m/z* 763 $(M+Na)^+$.

**Reveromycin L (15).** (2.4%). ESI(±)MS (100 kV) *m/z* 735 $(M+Na)^+$, 711 $(M–H)^-$. HRESI(–)MS *m/z* 711.3354 $(M–H)^-$ (calcd for $C_{39}H_{51}O_{12}$, 711.3381).

**Reveromycin M (16).** (1.6%). ESI(±)MS (100 kV) *m/z* 749 $(M+Na)^+$, 725 $(M–H)^-$. HRESI(+)MS *m/z* 749.3495 $(M+Na)^+$ (calcd for $C_{40}H_{54}O_{12}Na$, 749.3513).

## Acknowledgements

We thank M. Conte (IMB, UQ) for cytotoxicity screening. DNA sequencing was performed by the Australian Genome Research Facility. L.F. and M.F. acknowledge the provision of Australian Postgraduate Awards, and Z.K. the provision of a University of Queensland International Postgraduate Student Award. This research was funded, in part, by the Australian Research Council (ARC LP0989954), Novartis Animal Health Australasia, the Institute for Molecular Bioscience and The University of Queensland.

## References

1 H. Osada, H. Koshino, K. Isono, H. Takahashi and G. Kawanishi, *J. Antibiot.*, 1991, **44**, 259–261.
2 H. Takahashi, H. Osada, H. Koshino, T. Kudo, S. Amano, S. Shimizu, M. Yoshihama and K. Isono, *J. Antibiot.*, 1992, **45**, 1409–1413.
3 H. Takahashi, H. Osada, H. Koshino, M. Sasaki, R. Onose, M. Nakakoshi, M. Yoshihama and K. Isono, *J. Antibiot.*, 1992, **45**, 1414–1419.
4 H. Koshino, H. Takahashi, H. Osada and K. Isono, *J. Antibiot.*, 1992, **45**, 1420–1427.
5 M. Ubukata, H. Koshino, H. Osada and K. Isono, *J. Chem. Soc., Chem. Comm.*, 1994, 1877–1878.
6 T. Shimizu, T. Masuda, K. Hiramoto and T. Nakata, *Org. Lett.*, 2000, **2**, 2153–2156.
7 M. El Sous, D. Ganame, P. A. Tregloan and M. A. Rizzacasa, *Org. Lett.*, 2004, **6**, 3001–3004.
8 K. E. Drouet and E. A. Theodorakis, *J. Am. Chem. Soc.*, 1999, **121**, 456–457.
9 K. E. Drouet and E. A. Theodorakis, *Chem.–Eur. J.*, 2000, **6**, 1987–2001.
10 T. Masuda, K. Osako, T. Shimizu and T. Nakata, *Org. Lett.*, 1999, **1**, 941–944.
11 A. N. Cuzzupe, C. A. Hutton, M. J. Lilly, R. K. Mann, M. A. Rizzacasa and S. C. Zammit, *Org. Lett.*, 2000, **2**, 191–194.
12 A. N. Cuzzupe, C. A. Hutton, M. J. Lilly, R. K. Mann, K. J. McRae, S. C. Zammit and M. A. Rizzacasa, *J. Org. Chem.*, 2001, **66**, 2382–2393.
13 T. Shimizu, T. Usui, K. Machida, K. Furuya, H. Osada and T. Nakata, *Bioorg. Med. Chem. Lett.*, 2002, **12**, 3363–3366.
14 T. Shimizu, T. Usui, M. Fujikura, M. Kawatani, T. Satoh, K. Machida, N. Kanoh, J. T. Woo, H. Osada and M. Sodeoka, *Bioorg. Med. Chem. Lett.*, 2008, **18**, 3756–3760.
15 C. K. Jung, J. C. Wang and M. J. Krische, *J. Am. Chem. Soc.*, 2004, **126**, 4118–4119.
16 F. E. Wolter, K. Schneider, B. P. Davies, E. R. Socher, G. Nicholson, O. Seitz and R. D. Sussmuth, *Org. Lett.*, 2009, **11**, 2804–2807.
17 S. J. Moss, I. Carletti, C. Olano, R. M. Sheridan, M. Ward, V. Math, M. Nur-E-Alam, A. F. Braña, M. Q. Zhang, P. F. Leadlay, C. Méndez, J. A. Salas and B. Wilkinson, *J. Chem. Soc., Chem. Comm.*, 2006, 2341–2343.
18 A. Höltzel, C. Kempter, J. W. Metzger, G. Jung, I. Groth, T. Fritz and H.-P. Fiedler, *J. Antibiot.*, 1998, **51**, 699–707.
19 M. Lacroix, *Int. J. Cancer*, 2008, **122**, 1–4.
20 J. T. Woo, M. Kawatani, M. Kato, T. Shinki, T. Yonezawa, N. Kanoh, H. Nakagawa, M. Takamia, K. H. Lee, P. H. Stern, K. Nagai and H. Osada, *Proc. Natl. Acad. Sci. U. S. A.*, 2006, **103**, 4729–4734.
21 H. Muguruma, S. J. Yano, S. Kakiuchi, H. Uehara, M. Kawatani, H. Osada and S. Sone, *Clin. Cancer Res.*, 2005, **11**, 8822–8828.